CAMBRIDGE UNIVERSITY PRESS

RESEARCH ARTICLE

Numerical computation of the eigenvalues of the Broer–Kaup system for non-capillary waves

Peter J. Prins¹ D, Patrik V. Nabelek², Brandon M. Young² and Sander Wahls³ D

¹Delft Center for Systems and Control (DCSC), Delft University of Technology, Delft, The Netherlands

Corresponding author: Sander Wahls; Email: sander.wahls@kit.edu

Keywords: Broer-Kaup system; Non-linear Fourier Transform (NFT); Reflection analysis; Shallow water waves; Solitons

MSC Codes: Primary 65P99; Secondary 35P25

(Received 30 March 2025; revised 4 July 2025; accepted 18 August 2025)

Abstract

We present an algorithm to compute the eigenvalues of the Broer–Kaup (BK) system. The BK system is a system of non-linear partial differential equations that can be used as a model for weakly non-linear wave phenomena in 1+1 dimensions, such as shallow water waves in a flume. It can be seen as the natural generalization of the more familiar Korteweg–de Vries (KdV) equation. Whereas the KdV equation is only valid for waves propagating in one direction, the BK system covers waves moving simultaneously in both directions. This makes the BK system the natural candidate model for reflection analysis in shallow water conditions. Analogous to the KdV equation, the eigenvalues of the BK system each characterize a soliton, which can be moving forward or backward. In this paper, we show how the eigenvalues can be computed numerically from free surface data. Under mild and verifiable conditions, we can apply quasi Sturm–Liouville oscillation theory to guarantee that every soliton is found.

1. Introduction

The Broer–Kaup (BK) system is a Boussinesq-type partial differential equation (PDE) that describes certain weakly non-linear wave phenomena in one space dimension. It was independently derived in [7, Eqs. (3.2)–(3.3)] and [18] as a model for shallow water waves. Whereas the more familiar Korteweg–de Vries (KdV) equation only allows unidirectional waves, the BK system allows waves to move simultaneously in both directions. Even though the BK system is a Boussinesq-type equation, it should not be confused with the so-called Boussinesq one equation. The latter equation mathematically allows forward and backward propagating waves. It is however not a valid model for bidirectional water waves, most fundamentally because Boussinesq assumed unidirectionality in its derivation [27, p. 134], [46, p. 291], [47, §V], [10].

The BK system provides a good approximation of the full water wave problem for sufficiently smooth small-amplitude long-wavelength solutions, but it is in general ill-posed [4, p. 1175]. At this point, it is important to understand that the ill-posedness results from a *short-wave* instability. Hence, the instability ceases to be a concern when the BK system is used to model *long waves* provided no significant variations on short length scales are observed in the solutions considered. The rigorous justification of the BK system as a valid asymptotic model of shallow water waves in the long wave limit was given in [21]; see remark 6.25 in particular. The BK system was derived rigorously as an asymptotic

© The Author(s), 2025. Published by Cambridge University Press. This is an Open Access article, distributed under the terms of the Creative Commons Attribution licence (http://creativecommons.org/licenses/by/4.0), which permits unrestricted re-use, distribution and reproduction, provided the original article is properly cited.

²Department of Mathematics, Oregon State University, Corvallis, OR, USA

³Institute of Industrial Information Technology, Karlsruhe Institute of Technology, Karlsruhe, Germany P. J. Prins mostly worked on this manuscript when he was still with DCSC. He left DCSC in 2022.

Prins et al.

2

description of the Benjamin equation for an interfacial internal wave in the long wave limit in [11]. An analysis of the conservation laws and a filtered pseudo-spectral method for the numerical approximation of solutions to the BK system were provided by [3]. The BK system was also used to model undular bores in [16], where also Whitham modulation equations were derived. An up to date summary of mathematical results on the BK system can be found in the recent review paper [19]. On the experimental side, two solutions of the BK system –a two-soliton head-on interaction and a two-soliton overtaking interaction—were recently verified in a wave flume [38]. Thus, there is reason to believe that the well-behaved solutions of the BK system can be of practical interest. This point was also made in [29], where an analytical method to compute a large class of well-behaved solutions of the BK system was presented. For similar reasons, [28] also argues that the BK system is an interesting candidate for certain engineering applications.

Like the KdV equation, the BK system is integrable, meaning that its initial value problem can be solved using the inverse scattering method [18, 20, 39]. The forward transform in the inverse scattering method is nowadays often referred to as Non-linear Fourier Transform (NFT) for reasons first pointed out in [1]. NFTs are not only a tool to solve integrable PDEs; like the conventional Fourier transform, they can decompose space or time series into physically meaningful components. In particular, they reveal potentially hidden solitons in time or space series [2]. This makes them interesting tools for non-linear signal processing problems. In the context of shallow water waves, various authors have already exploited the KdV-NFT to detect hidden solitons in data. See, e.g., [8, 9, 25, 30, 32, 33, 41–43]. NFTs are particularly useful for the analysis of so-called soliton gases, which occur when the dynamics are dominated by many – typically hidden – interacting solitons [40]. Recently, a kinetic description of the density of states of a soliton gas described by the BK system was given in [15].

Similar to other NFTs, the BK-NFT decomposes free surface data into solitons and other non-linear wave components. In contrast to the KdV-NFT, it can deal with both forward and backward moving solitons in shallow water. More specifically, the BK-NFT spectrum is divided into a discrete part and a continuous part, where the discrete part is associated to the potentially hidden solitons in the space series of interest. The discrete part in turn consists of pairs of eigenvalues and norming constants, with each pair describing a single soliton. The eigenvalues provide the direction, amplitude and speed of the associated solitons, while the norming constants provide phase shifts. The eigenvalues in the BK-NFT are hence of interest for reflection analysis of shallow water waves. However, to the best of our knowledge, so far no numerical method to compute the eigenvalues from given data has been proposed. In this paper, we therefore present an algorithm to compute the eigenvalues numerically.

The remainder of the paper is structured as follows. In Section 2, the BK system, its soliton solution and the eigenvalues in its NFT are introduced. The Sections 3 and 4 describe the proposed numerical method for second and fourth order accuracy, respectively. The proposed algorithm is validated in Section 5 on two numerical examples. Finally, the paper is concluded in Section 6.

2. Preliminaries

In this section, we briefly introduce the BK system and its soliton solution. Furthermore, the definition of the eigenvalues of the BK-NFT spectrum is provided.

2.1. The BK system

When the BK system is used to model water waves over a flat bottom it has the following form [7, Eqs. (3.2)–(3.3)], [29, Eqs. (1)–(2)].

¹More specifically, the BK system can be rewritten to fit the AKNS framework [39, §6.3], [47, §III], [26].

$$\begin{bmatrix} \eta \\ \upsilon \end{bmatrix}_{\tilde{t}} = - \begin{bmatrix} (h_0 + \eta)\upsilon + \alpha h_0 \upsilon_{\tilde{x}\tilde{x}} \\ g\eta + \frac{1}{2}\upsilon^2 \end{bmatrix}_{\tilde{x}}, \tag{2.1}$$

where \tilde{x} [m] is the horizontal position, \tilde{t} [s] is the time, $\eta(\tilde{x}, \tilde{t})$ [m] is the free surface elevation with respect to the still water level, $\upsilon(\tilde{x}, \tilde{t})$ [m s⁻¹] is the horizontal particle velocity at the free surface, h_0 [m] is the still water level, τ [N m⁻¹] is the surface tension of the water, ρ [kg m⁻³] is the water density, g [m s⁻²] is the gravitational acceleration, and α [m²] := $h_0^2/3 - \tau/(\rho g)$.

Note that subscripts containing function arguments indicate partial derivatives. For example, $v_{\tilde{x}\tilde{x}} = \frac{\partial^2 v}{\partial \tilde{x}^2}$. Since the discrete spectrum of capillary waves differs from ordinary, non-capillary waves [18, §2], we will assume non-capillary waves throughout this paper. That is, $\alpha > 0$ m².

The normalization

$$w := (h_0 + \eta)/h_0 \ge 0, (2.2)$$

$$u := \upsilon / \sqrt{gh_0} \in \mathbb{R},\tag{2.3}$$

$$x := \tilde{x}/\sqrt{\alpha} \in \mathbb{R},\tag{2.4}$$

$$t := \tilde{t}/\sqrt{\alpha/(gh_0)} \in \mathbb{R} \tag{2.5}$$

results in the normalized BK system [39, Eq. (2)]

$$\begin{bmatrix} w \\ u \end{bmatrix}_t = - \begin{bmatrix} wu + u_{xx} \\ w + \frac{1}{2}u^2 \end{bmatrix}_x.$$
 (2.6)

The same normalized equation can be obtained for the formulation of the BK system in [18] by letting $\pi = w - 1$ and $\Phi_x = u$ before reversing the sign of x and choosing $\epsilon = -1$ and $\beta = 1$.

The BK system is invariant under the following scale transformation. If $w(x,t) = w_0(x,t)$, $u(x,t) = u_0(x,t)$ is any solution of Eq. (2.6) and d is any non-zero real constant, then $w(x,t) = d^2w_0(dx,d^2t)$, $u(x,t) = du_0(dx,d^2t)$ is also a solution. In particular, by choosing d = -1 it follows that the BK system is symmetric with respect to the wave direction.

2.2. The soliton solution of the BK equation

The soliton solution of the normalized BK system in Eq. (2.6) can be written as

$$\begin{cases} w(x,t) = 1 + 2\kappa^2 \operatorname{sech}^2(\theta(x,t) - \beta) + 2\kappa^2 \operatorname{sech}^2(\theta(x,t) + \beta) \\ u(x,t) = \frac{4\kappa^2 \operatorname{sign}(c)}{\cosh^2(\theta(x,t)) + \frac{1}{2}(|c| - 1)} \end{cases}, \tag{2.7}$$

where

$$\theta(x,t) := \kappa(x - ct) - \varphi, \tag{2.8}$$

$$\kappa = \frac{1}{2}\sqrt{c^2 - 1},\tag{2.9}$$

$$\beta := \frac{1}{2} \ln (|c| - 2\kappa),$$
 (2.10)

$$c \in \{c \in \mathbb{R} \mid |c| \ge 1\},\tag{2.11}$$

$$\varphi \in \mathbb{R} \tag{2.12}$$

and sign(c) = -1 if c < 0, sign(0) = 0 and sign(c) = +1 if c > 0. The free parameters are the phase offset φ and the normalized celerity c. Here, the celerity is positive for waves that move to the right and

4 Prins et al.

negative for waves that move to the left. We remark that the representation of the BK system used in [18] defines x with a reversed sign compared to the physical BK system and by that switches left and right moving waves. For |c| > 2, Eq. (2.7) becomes a double crested wave [47, §II], which might be surprising in view of physical considerations. However, if |c| > 2, the amplitude of the free surface elevation is greater than twice the still water level $(w > 3 \Leftrightarrow \eta > 2h_0)$. That amplitude is too large for a shallow water wave and hence the BK system is not an adequate model for such waves in the first place. For shallow water waves |c| < 2, and Eq. (2.7) describes a single crested wave.

The eigenvalues of the BK-NFT spectrum

In the inverse scattering method, the NFT associated to an integrable equation is derived from the spectrum of the first operator in the corresponding Lax pair. For the BK system, we need to solve the spectral problem [18, Eq. (2.1)]

$$f_{xx}(x,t,c) = -Q(x,t,c)f(x,t,c),$$
 (2.13)

where

$$Q(x,t,c) := -\frac{1}{4} \left(c - \frac{u(x,t)}{2} - \sqrt{w(x,t)} \right) \left(c - \frac{u(x,t)}{2} + \sqrt{w(x,t)} \right) \in \mathbb{R}. \tag{2.14}$$

Here we have chosen to use the normalized celerity c as the spectral parameter. However, we will write κ meaning $\kappa(c) = \frac{1}{2}\sqrt{c^2 - 1}$ whenever it allows us to write equations more compactly. Since the spectrum does not depend on the fixed value of the time t, we omit the dependence on t from here on. The eigenvalues are the c for which the spectral problem admits a square integrable solution f. To localize the eigenvalues, typically scattering theory is utilized. We now outline the procedure for the BK-NFT. We assume that both u(x) and w(x,t) - 1 satisfy vanishing boundary conditions, ² to wit

$$\int_{-\infty}^{\infty} |u(x)|(1+|x|)\mathrm{d}x < \infty, \qquad \qquad \int_{-\infty}^{\infty} |w(x)-1|(1+|x|)\mathrm{d}x < \infty.$$

Then we can define two sets of linearly independent Jost solutions of Eq. (2.13) by the boundary conditions [18, Eq. (2.9)]

$$\begin{cases} \phi(x,c) \to \exp(\kappa x) \\ \bar{\phi}(x,c) \to \exp(-\kappa x) \end{cases} \quad \text{as } x \to -\infty,$$

$$\begin{cases} \bar{\psi}(x,c) \to \exp(\kappa x) \\ \psi(x,c) \to \exp(-\kappa x) \end{cases} \quad \text{as } x \to +\infty.$$

$$(2.15)$$

$$\begin{cases} \bar{\psi}(x,c) \to \exp(\kappa x) \\ \psi(x,c) \to \exp(-\kappa x) \end{cases} \text{ as } x \to +\infty.$$
 (2.16)

The coefficients that express one set of Jost solutions as a linear combination of the other are known as the scattering parameters. These are implicitly defined by [18, Eq. (2.11)]

$$\begin{bmatrix} \phi(x,c) & \bar{\phi}(x,c) \end{bmatrix} = \begin{bmatrix} \bar{\psi}(x,c) & \psi(x,c) \end{bmatrix} \underbrace{\begin{bmatrix} a(c) & \bar{b}(c) \\ b(c) & \bar{a}(c) \end{bmatrix}}_{=:S(c)}.$$
 (2.17)

Finally, the eigenvalues of the BK system are the values $c = c_n$ for which $a(c_n) = 0$, or equivalently $\phi(x,c_n) \propto \psi(x,c_n)$. This can be seen as follows. We can write any solution of Eq. (2.13) as a linear

transformed before proceeding, see Section 2.1.

²If instead $w(x,t) - d^{-2}$ satisfies the vanishing boundary conditions for another real constant $d \notin \{0,1\}$ the data should be appropriately scale

combination of any set of Jost solutions: $f(x,c) = \alpha \phi(x,c) + \beta \bar{\phi}(x,c) = \gamma \bar{\psi}(x,c) + \delta \psi(x,c)$. A solution f is an eigenfunction if and only if it is square-integrable. In light of (2.15)–(2.16), this is equivalent to

$$f(x,c) = \alpha \phi(x,c) = \delta \psi(x,c), \quad \alpha, \delta \neq 0.$$
 (2.18)

Eigenvalues in the interval $(1, \infty)$ each correspond to a soliton that moves to the right, whereas eigenvalues in the interval $(-\infty, -1)$ each correspond to a soliton that moves to the left [18, p. 406]. The single soliton solution (2.7) leads to exactly one eigenvalue. *N*-soliton solutions are similarly characterized by *N* eigenvalues [47]. The continuous part of the NFT is zero for *N*-solitons.

Remark 2.1. The fact that no eigenvalues exist for which $|c| \le 1$ should be no surprise if we think of the BK system as a bidirectional generalization of the KdV equation. For the KdV equation it is well known that all solitons move faster than $\sqrt{gh_0}$. The condition |c| > 1 means that for the BK system too no soliton can have a physical celerity between $-\sqrt{gh_0}$ and $\sqrt{gh_0}$.

Remark 2.2. Besides the eigenvalues, the discrete part of the BK-NFT also contains corresponding norming constants $b(c_n)$, which specify the phases of the solitons. Their numerical computation is not considered in this paper. Instead we refer to [35] for a possible approach.

3. Numerical computation of eigenvalues of the BK system

In this section, we assume that we are given samples of wave data $w(x) = w(x, t_0)$ and $u(x) = u(x, t_0)$, where t_0 is some point in time, and that we want to compute the eigenvalues of the BK system for that data. For other PDEs that are solvable by NFTs, this problem has often been discussed in the literature, e.g. [6, 12–14, 31, 35, 36, 44, 45]. Furthermore there exists a rich body of work on the numerical computation of eigenvalues of Sturm–Liouville (SL) equations, which can be applied if the spectral problem of such a PDE (cf. Eq. (2.13)) happens to be a SL equation. See e.g. [5, 22, 24] and [23, Ch. 2] for a survey of earlier methods.

Our approach will be to adapt the recent algorithm for the eigenvalues of the KdV equation from [36] to the BK case. A high-level overview of our proposed method follows.

- **Input:** Samples $u(x_k)$ and $w(x_k)$ on an equidistant grid x_1, \ldots, x_D
- Output: BK eigenvalues $c_{L1}, \ldots, c_{LN_L} \in (-\infty, -1)$ and $c_{R1}, \ldots, c_{RN_R} \in (1, \infty)$
- Verify that the data satisfies certain applicability conditions
- Determine the eigenvalues in $(-\infty, -1)$ with a modified version of [36]
- Determine the eigenvalues in $(1, \infty)$ with a modified version of [36]

The algorithm in [36] combines reliable bracketing of the eigenvalues based on SL oscillation theory (e.g. [34, 37]) with quickly converging Newton–Raphson (NR) refinements. The spectral problem of the BK system is *not* a classic SL problem, which means that the results from classic SL oscillation theory used in [36] cannot be exploited in the BK case. However, we will show that the relevant results can be replaced in the BK case when the eigenvalues of left and right moving solitons are considered separately, and two applicability conditions that can be checked from the data and which are usually satisfied for shallow water wave data are fulfilled.

The following aspects of the algorithm in [36] need to be revisited before it can be applied to the BK system as outlined above.

- Computation of bounds on the eigenvalues to reduce the search spaces to finite intervals.
- Verification of the relevant results from oscillation theory for the BK system.
- Numerical computation of the so-called accounting function (for bracketing of eigenvalues).

• Numerical computation of the so-called scattering parameter a(c) and its derivative (for NR refinements of approximate eigenvalues).

These points will be addressed one by one below, after our assumptions on the data have been introduced.

Applicability conditions *3.1*.

The spectral problem of the BK system Eq. (2.13) is not a classic SL equation, because Q(x,c) is not an affine function of any suitably chosen spectral parameter. However, we will show that under the assumption |u(x)| < 2 for all x, a result from generalized SL theory can be applied. This condition is unlikely to be violated while using the BK system to model shallow water waves, since $|u| \ge 2$ physically corresponds to a particle velocity of $v \ge 2\sqrt{gh_0}$, so at least twice the still water celerity. The single soliton solution Eq. (2.7) breaks this bound if and only if it is double-crested. As discussed earlier, the double crested soliton lies beyond the regime in which the BK system is an adequate model for shallow water waves. We shall furthermore assume that w(x) is bounded, which is certainly true for any real-world wave data. Both conditions can be verified from the data before proceeding.

3.2. Bounds on the eigenvalues

Regardless of the data w(x), u(x), every eigenvalue of the BK system Eq. (2.6) satisfies $|c_n| > 1$ [18, p. 406]. For given data, we can furthermore compute upper bounds on |c| for the left and right moving part of the discrete spectrum as follows. Recall that eigenfunctions satisfy Eq. (2.18). Without loss of generality, we assume $\alpha = 1$, so that f(x, c) > 0 and $f_x(x, c) > 0$ for x sufficiently close to $-\infty$ by (2.15). If now Q(x,c) were negative for all x, then by Eq. (2.13) $f_{xx}(x,c) > 0$ for all x. Therefore the function f(x,c) would be monotonously increasing for all x, which is incompatible with square-integrability. Hence c cannot be an eigenvalue if Q(x,c) < 0 for all x. This, together with Eq. (2.14), implies that $c \in (c_{lb}, -1)$ for the left moving part and $c \in (1, c_{ub})$ for the right moving part of the discrete spectrum, where

$$c_{\rm lb} = \inf_{x} \frac{1}{2} u(x) - \sqrt{w(x)},$$
 (3.1)

$$c_{\text{lb}} = \inf_{x} \frac{1}{2}u(x) - \sqrt{w(x)},$$

$$c_{\text{ub}} = \sup_{x} \frac{1}{2}u(x) + \sqrt{w(x)}.$$
(3.1)

These bounds can be computed from the data and reduce the search space from two half lines to two finite (or even empty) intervals.

Oscillation theory for the BK system

The accounting function is defined as

$$s(c) := \text{number of zero-crossings in } \phi(x, c) \text{ for } -\infty < x < \infty$$
 (3.3)

and satisfies

$$s(c) = \text{number of eigenvalues in } \begin{cases} [1, c), & c \in (1, c_{\text{ub}}) \\ (c, -1], & c \in (c_{\text{lb}}, -1) \end{cases}$$
 (3.4)

By using bracketing to localize the jump points of s(c), we can find arbitrarily small intervals around each eigenvalue. We now discuss how Eq. (3.4) follows from [17, Thm. 2.1].

Let us assume that u(x) has compact support, which is an implicit assumption underlying the numerical method anyway. Without loss of generality, we assume that u(x) = 0 and w(x) = 1 for $x \notin [0, 1]$.

Due to Eq. (2.18), any eigenfunction must fulfill the boundary condition for ϕ in (2.15) at the left end of the support, and the boundary condition for ψ in (2.16) at the right end of the support. That is,

$$f(0,c) = \alpha, \quad f_x(0,c) = \alpha \kappa, \quad f(1,c) = \beta, \quad f_x(1,c) = -\beta \kappa.$$
 (3.5)

The spectral problem for the BK system can thus be written in the form

$$[P(x,c)f_x]_x + Q(x,c)f = 0, \quad x \in [0,1], \tag{3.6}$$

$$\alpha_0(c)f(0,c) + \beta_0(c)f_x(0,c) = 0, (3.7)$$

$$\alpha_1(c)f(1,c) + \beta_1(c)f_x(1,c) = 0, (3.8)$$

where P(x, c) := 1, $\alpha_0(c) := -\kappa$, $\beta_0(c) := 1$, $\alpha_1(c) := \kappa$ and $\beta_1(c) := 1$. This kind of spectral problem has been considered in [17]. We now verify that the relevant assumptions in [17] are fulfilled for the reformulated BK spectral problem if $c \in (1, c_{ub})$.

- Standard assumptions (S1)–(S5): These are fulfilled as soon as u(x) and w(x) are piecewise continuous. (Note that Remark 1 in [17] clarifies that S1 can be weakened.)
- Monotonicity assumptions (M1)-(M4): The applicability conditions in Section 3.1 ensure that Q(x,c) is strictly increasing in c on $(1,c_{ub})$. The monotonicity conditions are therefore fulfilled.
- Limit assumption (L3): We have $\alpha_0(c_{ub})\beta_0(c_{ub}) = -\kappa \le 0$ and $\alpha_1(c_{ub})\beta_1(c_{ub}) = \kappa \ge 0$. The discussion in Section 3.2 furthermore showed that $Q(x, c_{ub}) \le 0$ for all $x \in [0, 1]$.
- We have $\bar{f}(c) := \alpha_1(c)f(1,c) + \beta_1(c)f_x(1,c) = \kappa\beta + 1(-\beta\kappa) = 0$.

The first case in Eq. (3.4) now follows from Part 3 of Theorem 2.1 in [17] for $c \in (1, c_{ub})$. The case $c \in (c_{lb}, -1)$ follows similarly using the remark on p. 928 of that paper.

3.4. Numerical computation of the accounting function

Numerically, the accounting function is attractive as it can be computed exactly subject to the numerical discretization in a simple way. The numerically computed accounting function increases by one exactly at the "numerical" eigenvalues and is constant otherwise. This property ensures that we localize *all* eigenvalues. In contrast, algorithms that are based on finding the zeros of a(c) directly can miss closely spaced eigenvalues. This has been discussed in detail in [36] for the spectral problem of the KdV equation. Conveniently, the only change that is needed to adapt the discussion and computation of the accounting function to the BK case is to replace $q_d - \kappa^2$, where $q_d := q(x_d)$, throughout by $Q(x_d, c)$, in particular $\gamma := \sqrt{Q(x_d, c)}$. To see this, note that the first-order representation

$$\begin{bmatrix} \phi(x,c) \\ \phi_x(x,c) \end{bmatrix}_x = \begin{bmatrix} 0 & 1 \\ \kappa^2 - q(x) & 0 \end{bmatrix} \begin{bmatrix} \phi(x,c) \\ \phi_x(x,c) \end{bmatrix}, \tag{3.9}$$

of the spectral problem for the KdV equation in [36, Eq. (2)] turns into a first-order representation of the BK spectral problem in Eq. (2.13) under this transformation.

3.5. Numerical computation of the Jost functions and the scattering matrix

We now discuss how the scattering matrix in Eq. (2.17) and its derivative can be computed numerically. Recall that the zeros of the top-left element of the scattering matrix are exactly the eigenvalues, which is why we can use the scattering matrix and its derivative to perform NR refinements of approximate eigenvalues. For numerical computations it is convenient to rewrite Eq. (2.13) as a system of first-order

equations. Furthermore we augment the system to also obtain the derivative of the scattering matrix with respect to c, cf. [6]. To that end we define an operator

$$\widetilde{\mathsf{V}}_{\mathsf{C}} := \begin{bmatrix} 1 & \frac{\partial}{\partial x} & \frac{\partial}{\partial c} & \frac{\partial^2}{\partial x \partial c} \end{bmatrix}^{\mathsf{T}}. \tag{3.10}$$

Then Eq. (2.13) can be written as

$$\frac{\partial}{\partial x}\widetilde{f}_{C}(x,c) = \widetilde{A}_{C}(x,c)\widetilde{f}_{C}(x,c), \tag{3.11}$$

where $f_{\mathbf{C}}(x,c) := V_{\mathbf{C}}f(x,c)$ and

$$\widetilde{A}_{C}(x,c) := \begin{bmatrix} 0 & 1 & 0 & 0 \\ -Q(x,c) & 0 & 0 & 0 \\ 0 & 0 & 0 & 1 \\ -Q_{c}(x,c) & 0 & -Q(x,c) & 0 \end{bmatrix},$$
(3.12)

where $Q_c(x,c) = \frac{1}{4}(2c - u(x))$. In the representation of Eq. (3.11), the boundary conditions of the Jost solutions can be written as

$$\widetilde{\Phi}_{C}(x,c) := \begin{bmatrix}
\phi(x,c) & \overline{\phi}(x,c) & 0 & 0 \\
\phi_{x}(x,c) & \overline{\phi}_{x}(x,c) & 0 & 0 \\
\phi_{c}(x,c) & \overline{\phi}_{c}(x,c) & \phi(x,c) & \overline{\phi}(x,c) \\
\phi_{xc}(x,c) & \overline{\phi}_{xc}(x,c) & \phi_{x}(x,c) & \overline{\phi}_{x}(x,c)
\end{bmatrix} \rightarrow \widetilde{T}_{E}^{C}(x,c) \text{ as } x \to -\infty, \tag{3.13}$$

$$\widetilde{\Psi}_{C}(x,c) := \begin{bmatrix}
\overline{\psi}(x,c) & \psi(x,c) & 0 & 0 \\
\overline{\psi}_{x}(x,c) & \psi_{x}(x,c) & 0 & 0 \\
\overline{\psi}_{c}(x,c) & \psi_{c}(x,c) & \overline{\psi}(x,c) & \psi(x,c) \\
\overline{\psi}_{xc}(x,c) & \psi_{xc}(x,c) & \overline{\psi}_{x}(x,c) & \psi_{x}(x,c)
\end{bmatrix} \rightarrow \widetilde{T}_{E}^{C}(x,c) \text{ as } x \to +\infty, \tag{3.14}$$

$$\widetilde{\Psi}_{C}(x,c) := \begin{bmatrix}
\bar{\psi}(x,c) & \psi(x,c) & 0 & 0 \\
\bar{\psi}_{x}(x,c) & \psi_{x}(x,c) & 0 & 0 \\
\bar{\psi}_{c}(x,c) & \psi_{c}(x,c) & \bar{\psi}(x,c) & \psi(x,c) \\
\bar{\psi}_{xc}(x,c) & \psi_{xc}(x,c) & \bar{\psi}_{x}(x,c) & \psi_{x}(x,c)
\end{bmatrix} \rightarrow \widetilde{T}_{E}^{C}(x,c) \text{ as } x \to +\infty,$$
(3.14)

where

$$\widetilde{T}_{\mathrm{E}}^{\mathrm{C}}(x,c) := \begin{bmatrix} T_{\mathrm{S}}^{\mathrm{C}}(c) & \begin{bmatrix} 0 & 0 \\ 0 & 0 \end{bmatrix} \\ \frac{\mathrm{d}}{\mathrm{d}c} T_{\mathrm{S}}^{\mathrm{C}}(c) & T_{\mathrm{S}}^{\mathrm{C}}(c) \end{bmatrix} \begin{bmatrix} T_{\mathrm{E}}^{\mathrm{S}}(x,c) & \begin{bmatrix} 0 & 0 \\ 0 & 0 \end{bmatrix} \\ \frac{\partial}{\partial c} T_{\mathrm{E}}^{\mathrm{S}}(x,c) & T_{\mathrm{E}}^{\mathrm{S}}(x,c) \end{bmatrix}, \tag{3.15}$$

$$\begin{split} T_{\mathrm{S}}^{\mathrm{C}}(c) &= \begin{bmatrix} 1 & 1 \\ \kappa & -\kappa \end{bmatrix}, & T_{\mathrm{E}}^{\mathrm{S}}(x,c) &= \begin{bmatrix} \exp(\kappa x) & 0 \\ 0 & \exp(-\kappa x) \end{bmatrix}, \\ \frac{\mathrm{d}}{\mathrm{d}c} T_{\mathrm{S}}^{\mathrm{C}}(c) &= \frac{c}{4\kappa} \begin{bmatrix} 0 & 0 \\ 1 & -1 \end{bmatrix}, & \frac{\partial}{\partial c} T_{\mathrm{E}}^{\mathrm{S}}(x,c) &= \frac{cx}{4\kappa} \begin{bmatrix} 1 & 0 \\ 0 & -1 \end{bmatrix} T_{\mathrm{E}}^{\mathrm{S}}(x,c). \end{split}$$

Since $\widetilde{\Psi}_{\mathbb{C}}(x,c)$ is invertible for |c|>1 by the linear independence of $\bar{\psi}(x,c)$ and $\psi(x,c)$, once $\widetilde{\Phi}_{\mathbb{C}}(x,c)$ and $\widetilde{\Psi}_{C}(x,c)$ are known for the same position x, the scattering matrix and its derivative with respect to c can be computed as

$$\begin{bmatrix} S(c) & \begin{bmatrix} 0 & 0 \\ 0 & 0 \end{bmatrix} \\ \frac{d}{dc}S(c) & S(c) \end{bmatrix} \equiv \widetilde{\mathcal{\Psi}}_{C}^{-1}(x,c)\widetilde{\boldsymbol{\Phi}}_{C}(x,c). \tag{3.16}$$

We remark that computation time can be saved by pre- and post-multiplying the expression above by suitable selection matrices to compute only the required values, e.g.

$$\begin{bmatrix} a(c) \\ \frac{\mathrm{d}}{\mathrm{d}c}a(c) \end{bmatrix} = \begin{pmatrix} \begin{bmatrix} 1 & 0 & 0 & 0 \\ 0 & 0 & 1 & 0 \end{bmatrix} \widetilde{\mathcal{Y}}_{\mathrm{C}}^{-1}(x,c) \end{pmatrix} \begin{pmatrix} \widetilde{\Phi}_{\mathrm{C}}(x,c) \begin{bmatrix} 1 & 0 & 0 & 0 \end{bmatrix}^{\mathsf{T}} \end{pmatrix}, \tag{3.17}$$

$$S(c) = \left(\begin{bmatrix} 1 & 0 & 0 & 0 \\ 0 & 1 & 0 & 0 \end{bmatrix} \widetilde{\mathcal{Y}}_{C}^{-1}(x, c) \right) \left(\widetilde{\Phi}_{C}(x, c) \begin{bmatrix} 1 & 0 & 0 & 0 \\ 0 & 1 & 0 & 0 \end{bmatrix}^{\mathsf{T}} \right). \tag{3.18}$$

At this point it remains to propagate $\widetilde{\Phi}_C(x,c)$ and $\widetilde{\Psi}_C(x,c)$ to the same position x. Firstly we truncate the data to a window $x \in [X_-, X_+]$. That is, we assume u(x) = 0 and w(x) = 1 for all $x \notin [X_-, X_+]$, such that $\widetilde{\Phi}_C(X_-,c) = \widetilde{T}_E^C(X_-,c)$ and $\widetilde{\Psi}_C(X_+,c) = \widetilde{T}_E^C(X_+,c)$. Secondly we solve Eq. (3.11) by the exponential midpoint rule. That is, we approximate u(x) and w(x) by piecewise constant functions. Let D be the number of piecewise constant steps, then the stepsize is $\varepsilon := (X_+ - X_-)/D$ and the midpoints are $x_d := X_- + (d - \frac{1}{2})\varepsilon$ for $d = 1, 2, \ldots, D$. In each step Eq. (3.11) can be solved exactly:

$$\widetilde{f}_{C}(x_d + \frac{\varepsilon}{2}, c) = \widetilde{H}_{C}(x_d, c)\widetilde{f}_{C}(x_d - \frac{\varepsilon}{2}, c), \tag{3.19}$$

where

$$\widetilde{H}_{\mathcal{C}}(x_d, c) := \begin{bmatrix} H_{\mathcal{C}}(x_d, c) & \begin{bmatrix} 0 & 0 \\ 0 & 0 \end{bmatrix} \\ \frac{\partial}{\partial c} H_{\mathcal{C}}(x_d, c) & H_{\mathcal{C}}(x_d, c) \end{bmatrix}, \tag{3.20}$$

$$H_{C}(x_{d},c) = \exp\left(\begin{bmatrix} 0 & 1 \\ -Q(x_{d},c) & 0 \end{bmatrix} \varepsilon\right) = \begin{bmatrix} \cos(\gamma \varepsilon) & \varepsilon \operatorname{sinc}(\gamma \varepsilon) \\ -\gamma \sin(\gamma \varepsilon) & \cos(\gamma \varepsilon) \end{bmatrix}, \tag{3.21}$$

$$\frac{\partial}{\partial c} H_{\rm C}(x_d,c) = \left(2c - u(x_d)\right) \frac{\varepsilon}{8} \begin{bmatrix} \varepsilon {\rm sinc}(\gamma \varepsilon) & \varepsilon^2 h(\gamma \varepsilon) \\ {\rm sinc}(\gamma \varepsilon) + \cos(\gamma \varepsilon) & \varepsilon {\rm sinc}(\gamma \varepsilon) \end{bmatrix}, \tag{3.22}$$

where $\gamma := \sqrt{Q(x_d, c)}$, and

$$\operatorname{sinc}(\vartheta) := \begin{cases} \sin(\vartheta)/\vartheta & \vartheta \neq 0 \\ 1 & \vartheta = 0 \end{cases}, \tag{3.23}$$

$$h(\vartheta) := \begin{cases} (\operatorname{sinc}(\vartheta) - \cos(\vartheta))/\vartheta^2 & \vartheta \neq 0, \\ 1/3 & \vartheta = 0 \end{cases}$$
(3.24)

$$= \sum_{m=0}^{\infty} \frac{(-1)^m \vartheta^{2m}}{(2m+1)! (2m+3)} = \frac{1}{3} - \frac{\vartheta^2}{30} + \frac{\vartheta^4}{840} - \frac{\vartheta^6}{45360} + \dots$$
 (3.25)

We will evaluate $h(\gamma \varepsilon)$ for $|\gamma \varepsilon| < 1$ by a truncated Taylor series expansion of order 17 (i.e. 9 non-zero terms) to prevent catastrophic cancellation near $\gamma \varepsilon = 0$. Finally we can propagate $\widetilde{\Phi}_{\mathbb{C}}(x,c)$ from $x = X_{-}$ to $x = X_{+}$ as

$$\widetilde{\Phi}_{\mathcal{C}}(X_{+},c) = \widetilde{H}_{\mathcal{C}}(x_{D},c)\widetilde{H}_{\mathcal{C}}(x_{D-1},c)\cdots\widetilde{H}_{\mathcal{C}}(x_{2},c)\widetilde{H}_{\mathcal{C}}(x_{1},c)\widetilde{\Phi}_{\mathcal{C}}(X_{-},c). \tag{3.26}$$

4. Upgrade to fourth-order accuracy

In [36, §3.4], it is shown that the accuracy of the eigenvalue algorithm can be improved from second to fourth-order accuracy without breaking the accurate computation of the accounting function. This also applies to the BK system, but the expressions become a bit more complicated because Q(x, c) is not an affine function of u(x) and w(x). From the more general equation [13, Eq. (22)], we can see that the fourth-order integrator consists of two matrix exponentials per step, each of which are similar to Eq. (3.21), where $Q(x_d, c)$ is replaced by a specific weighted average of $Q\left(x_d \pm \varepsilon/(2\sqrt{3}), c\right)$. A weighted average of two second degree polynomials is again a second degree polynomial. Hence, we can find values u_i and u_i such that the resulting polynomial is parametrized as Eq. (2.14) in each case. By straightforward algebra, we find that the analogue of [36, Eq. (23)] for the BK system is

$$\widetilde{H}_{C}(x_{d},c) \leftarrow \widetilde{H}_{C}(x_{d},c) \begin{vmatrix} u(x_{d}) \leftarrow \widecheck{u}_{2d} \\ w(x_{d}) \leftarrow \widecheck{w}_{2d} \\ \varepsilon \leftarrow \varepsilon/2 \end{vmatrix} \widetilde{H}_{C}(x_{d},c) \begin{vmatrix} u(x_{d}) \leftarrow \widecheck{u}_{2d-1} \\ w(x_{d}) \leftarrow \widecheck{w}_{2d-1} \\ \varepsilon \leftarrow \varepsilon/2 \end{vmatrix}, \tag{4.1}$$

where \leftarrow denotes substitution (in Eqs. (3.20), (3.21) and (3.22)) and

$$\begin{bmatrix} \check{u}_{2d-1} & \check{w}_{2d-1} \\ \check{u}_{2d} & \check{w}_{2d} \end{bmatrix} := \begin{bmatrix} \frac{1}{2} + \frac{1}{\sqrt{3}} & \frac{1}{2} - \frac{1}{\sqrt{3}} \\ \frac{1}{2} - \frac{1}{\sqrt{3}} & \frac{1}{2} + \frac{1}{\sqrt{3}} \end{bmatrix} \begin{bmatrix} u \left(x_d - \frac{\varepsilon}{2\sqrt{3}} \right) & w \left(x_d - \frac{\varepsilon}{2\sqrt{3}} \right) \\ u \left(x_d + \frac{\varepsilon}{2\sqrt{3}} \right) & w \left(x_d + \frac{\varepsilon}{2\sqrt{3}} \right) \end{bmatrix} + \dots \\ - \begin{bmatrix} 0 & \frac{1}{48} \\ 0 & \frac{1}{48} \end{bmatrix} \left(u \left(x_d - \frac{\varepsilon}{2\sqrt{3}} \right) - u \left(x_d + \frac{\varepsilon}{2\sqrt{3}} \right) \right)^2.$$

$$(4.2)$$

If u(x) and w(x) are only available as sampled data, the values $u\left(x_d \pm \varepsilon/(2\sqrt{3})\right)$ and $w\left(x_d \pm \varepsilon/(2\sqrt{3})\right)$ can be obtained by band-limited interpolation as proposed in [13]. We must however verify that $\check{w}_i \geq 0$ and $|\check{u}_i| < 2$ for $i = 1, 2, \dots 2D$, because band-limited interpolation does not necessarily preserve these bounds. If these conditions are fulfilled, the fourth-order method can be interpreted as giving the exact solution of the spectral problem of the BK system if u(x) and w(x) were two suitable piecewise continuous functions with step size $\varepsilon/2$, 2D steps, and levels given by the pre-processed samples \check{u}_i and \check{w}_i . Following this interpretation the computation of the accounting function remains the same as for the exponential midpoint rule.

5. Validation of the Method on Multi-Soliton Solutions

In this section, we validate convergence and accuracy of the numerical calculation of the eigenvalues when applied to exact multi-soliton solutions computed using the approach from [29]. Implementing the approach in Mathematica, we produced solutions for which we know the correct eigenvalues, and we can therefore study how accurate their recovery is at various times. We use these solutions to validate an implementation of the numerical method described in Sections 3 and 4 in MATLAB. We show the eigenvalues are consistently computed as time evolves, and that the eigenvalues are computed with fourth-order accuracy.

5.1. Multisoliton solutions of the BK system

The multi-soliton solutions are defined in terms of real parameters $\{\lambda_j\}_{j=1}^n$ satisfying $|\lambda_j| > 1$ and nonzero real parameters $\{b_j\}_{j=1}^n$ such that λ_j and b_j have the same sign. These parameters can be chosen freely subject to the given constraints. The eigenvalues are determined by λ_j according to the relationship $c_j = -\frac{1}{2}(\lambda_j + 1/\lambda_j)$ while b_j determines the phase of the jth soliton (and are therefore related to $b(c_j)$).

We can then form the matrix-valued function M(x, t) with entries

$$M_{ij}(x,t) = \delta_{ij} + \frac{b_i \lambda_i}{\lambda_i \lambda_j - 1} \exp\left(-(\lambda_i - \lambda_i^{-1})x - \frac{1}{2}(\lambda_i^2 - \lambda_i^{-2})t\right),\tag{5.1}$$

and the vector-valued function $\mathbf{y}(x, t)$ with entries

$$y_j(x,t) = b_j \exp\left(-(\lambda_i - \lambda_i^{-1})x - \frac{1}{2}(\lambda_i^2 - \lambda_i^{-2})t\right).$$
 (5.2)

Using the entries $f_i(x, t)$ in the unique solution $\mathbf{f}(x, t)$ to

$$M(x,t)\mathbf{f}(x,t) = \mathbf{y}(x,t),\tag{5.3}$$

we can produce solutions to the nondimensional version of the BK system from [29] using

$$\varphi(x,t) = -\log\left(1 - \sum_{j=1}^{n} \frac{f_j(x,t)}{\lambda_j}\right),\tag{5.4}$$

$$\eta(x,t) = -\frac{1}{2} \frac{\partial^2 \varphi}{\partial x^2}(x,t) - \sum_{j=1}^n \frac{\partial f_j}{\partial x}(x,t).$$
 (5.5)

The function $\varphi(x,t)$ has the interpretation of a velocity potential, so it makes sense to define the velocity $v(x,t) = \frac{\partial \varphi}{\partial x}(x,t)$. The solutions to the version of the Kaup-Broer solutions w(x,t) and u(x,t) to the BK system considered here can the be produced as

$$w(x,t) = \eta\left(\frac{x}{2}, \frac{t}{2}\right) + 1, \quad u(x,t) = v\left(\frac{x}{2}, \frac{t}{2}\right).$$
 (5.6)

The above formulas can be implemented symbolically, and this provides exact formulas for a class of solutions depending on the parameters λ_i and b_i for which the eigenvalues c_i are known.

5.2. Validation of a 5-soliton solution

We first validate the numerical computation of the eigenvalues on a 5-soliton solution w(x, t), u(x, t) to the BK system produced in Mathematica using the above approach with parameters λ_n and b_n given in Table 1.

The corresponding eigenvalues c_n for this solution were evaluated up to the accuracy of double precision floating-point numbers and are provided in in Table 1 as well. The 5-soliton synthetic data are shown in Figure 1 at times t = -50, t = 0 and t = 50 at 1001 equally spaced grid-points for $x \in$

Table 1. Parameters and eigenvalues of the 5-soliton solution.

λ_n	b_n	c_n
1.5	1	-1.08333333333333333
1.1	1	-1.0045454545454546
-1.1	-1	1.0045454545454546
-1.2	-1	1.0166666666666666
-1.35	-1	1.0453703703703705
	1.5 1.1 -1.1 -1.2	1.5 1 1.1 1 -1.1 -1 -1.2 -1

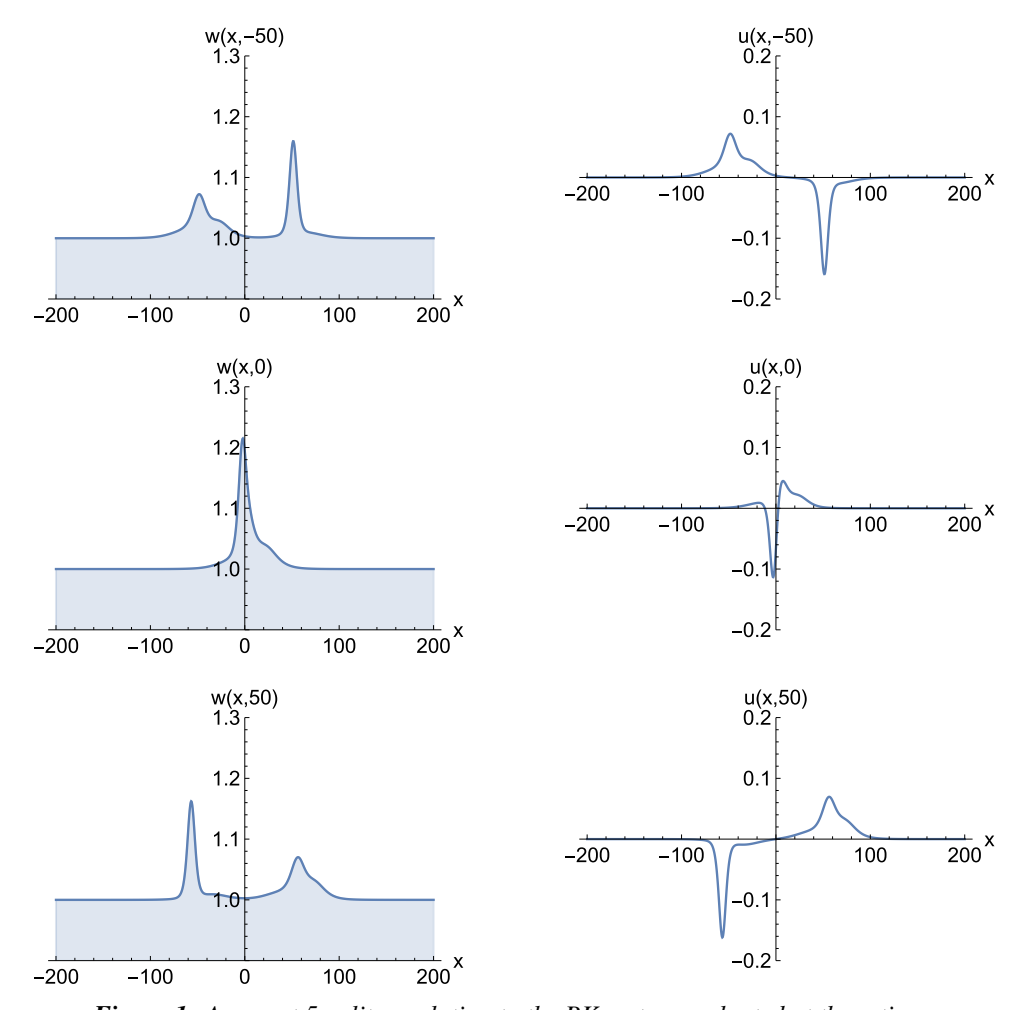


Figure 1. An exact 5-soliton solution to the BK system evaluated at three times

[-200, 200] with both endpoints included. The five eigenvalues detected by the numerical method are shown in Figure 2 as time evolves from t = -50 to t = 50 using 1001 grid-points at each time. We see that the computed eigenvalues are consistent and correct with at least 9 correct digits throughout the whole evolution from time t = -50 to time t = 50.

The variations occur due to three error sources. First, there is a discretization error because the signal is assumed to be piecewise constant during the derivation of the algorithm. This error can be reduced by decreasing the step size. Second, there is a truncation error because the signal is assumed to be zero outside the computational domain, which is only approximately true for the considered 5-soliton solutions. This error can be reduced by extending the computational domain (and using the same step size, which means more samples). Third, there is a finite precision error due to the limitations of floating-point arithmetic. This error can be reduced by the use of arbitrary precision floating-point numbers. However, the computational cost of the method will increase when any of these errors is reduced.

The theory discussed in the previous sections indicates that the algorithm should be fourth-order accurate, i.e. the error should be proportional to $(\Delta x)^4$, where Δx is the grid-spacing. We verify the accuracy order on the synthetic data produced from the exact 5-soliton solution. At time t = 0, the 5-soliton solution was evaluated on 2^{15} uniformly space grid-points on [-200, 200) with only the left endpoint included. This was then sub-sampled to produce synthetic data with 2^n grid-points for n = 1

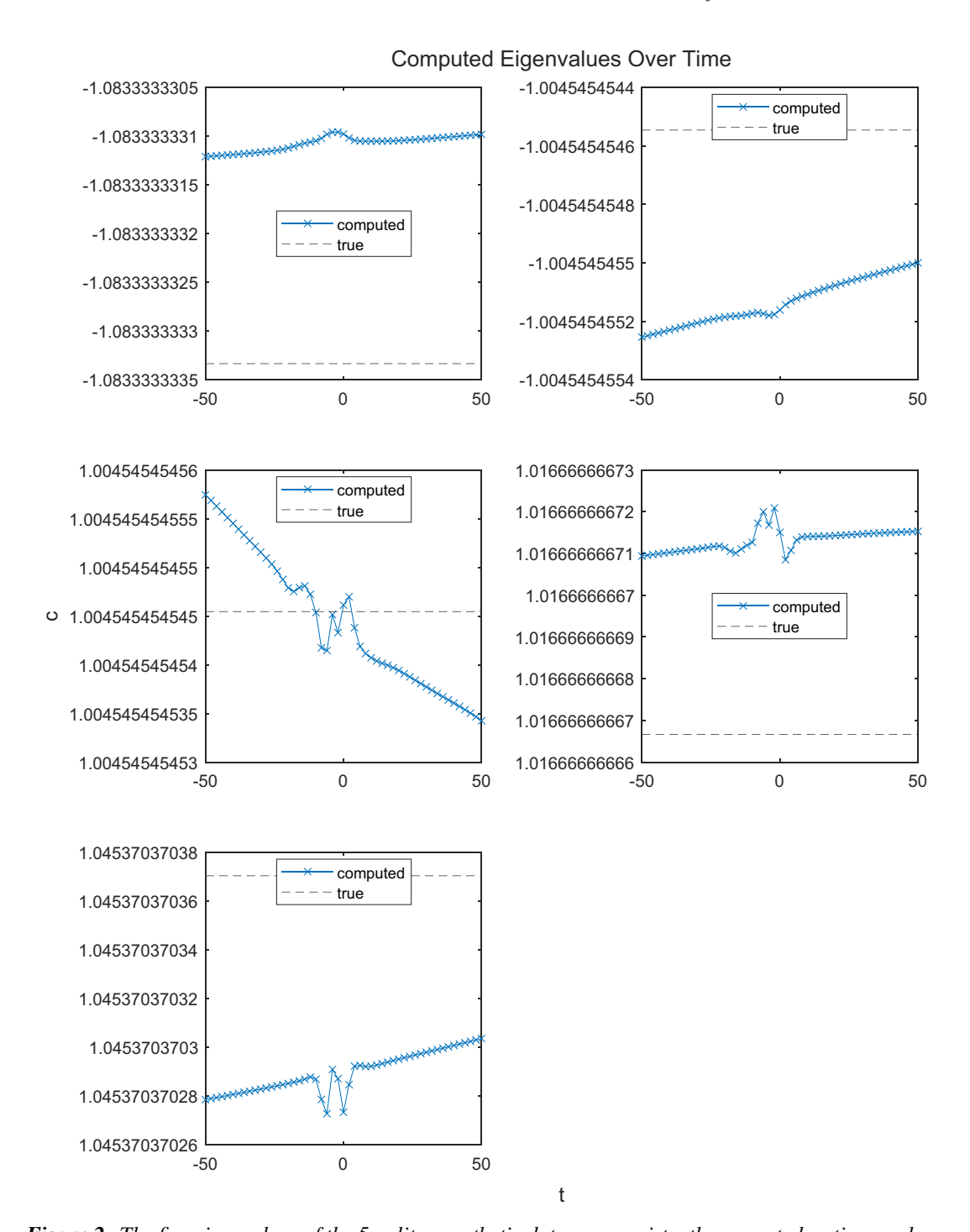


Figure 2. The five eigenvalues of the 5-soliton synthetic data are consistently computed as time evolves

15, 14, ..., 9 respectively. The absolute value of the errors in the computation of each of the 5 detected eigenvalues for various step sizes $\Delta x = 400/2^n$ on a log-log plot are shown in blue in Figure 3. For each eigenvalue, a line with the same slope as $(\Delta x)^4$ is also plotted, and we see that the rate of convergence is in good agreement with the predicted fourth-order convergence of the method.

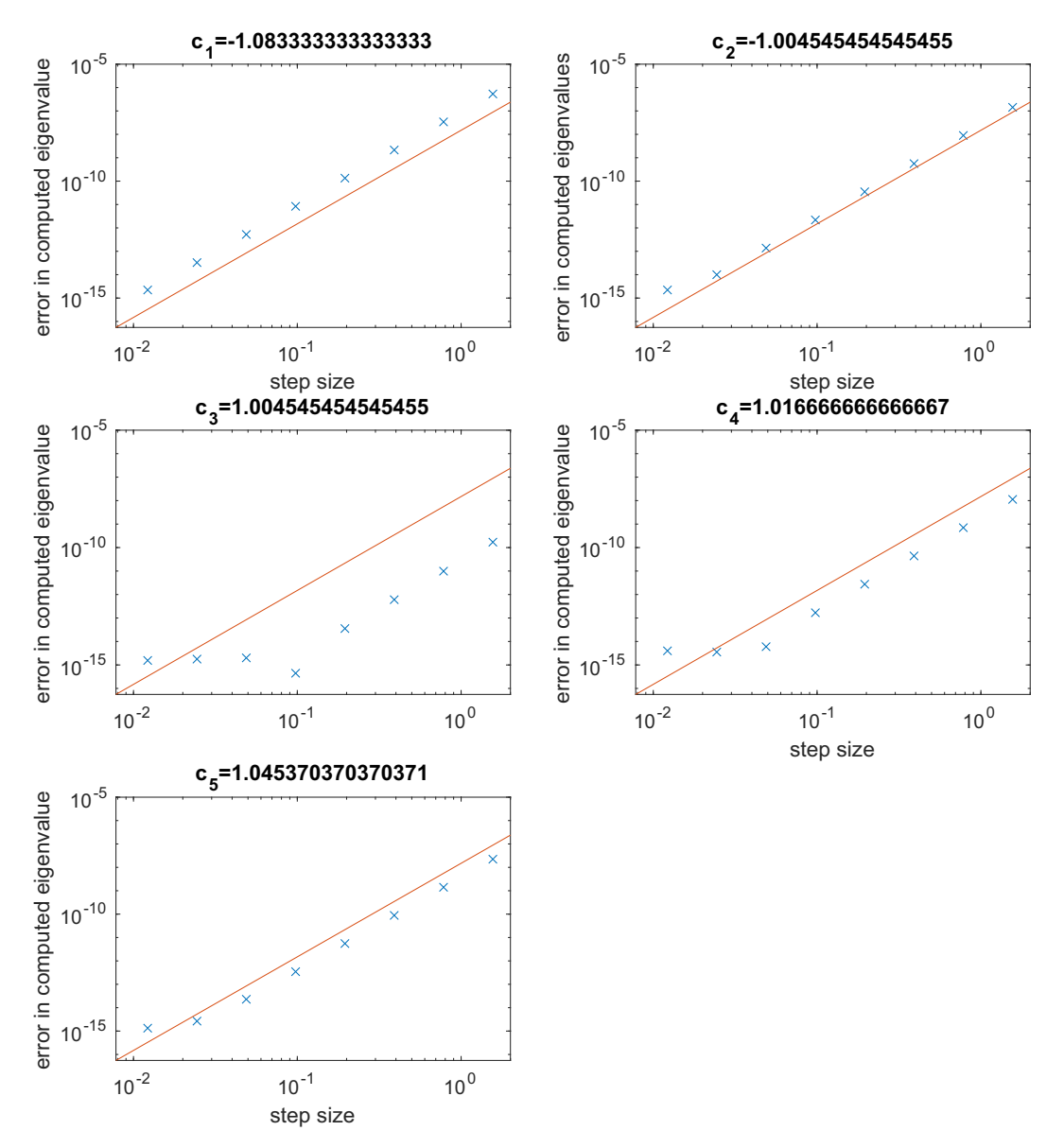


Figure 3. The computation of the five eigenvalues converge to machine precision with fourth-order accuracy

5.3. Validation of a 8-soliton solution

We also validated the numerical method for the eigenvalues using an 8-soliton solution with the parameters λ_n and b_n given in Table 2. The 8 eigenvalues c_n for this solution up to the accuracy of double precision floating-point numbers are also provided in Table 2. The 8-soliton synthetic data are shown in Figure 4 at times t = -20, t = 0, and t = 20 sampled on 1001 equally space grid-points for $x \in [-200, 200]$ with both endpoints. The eight eigenvalues detected by the algorithm as time evolves from t = -20 to t = 20 using 1001 grid-points at each time are shown in Figure 5. We see that the computed eigenvalues are correct with at least 8 correct digits throughout the whole evolution from time t = -20 to time t = 20. This again indicates the algorithm is accurate and can consistently detect the correct eigenvalues with good accuracy throughout the time evolution from time t = -20 to time t = 20.

\overline{n}	λ_n	b_n	c_n
1	1.5	1	-1.08333333333333333
2	1.4	1	-1.0571428571428572
3	1.3	1	-1.0346153846153845
4	1.1	1	-1.0045454545454546
5	-1.1	-1	1.0045454545454546
6	-1.2	-1	1.0166666666666666
7	-1.35	-1	1.0453703703703705
8	-1.45	-1	1.0698275862068964

Table 2. Parameters and eigenvalues of the 8-soliton solution.

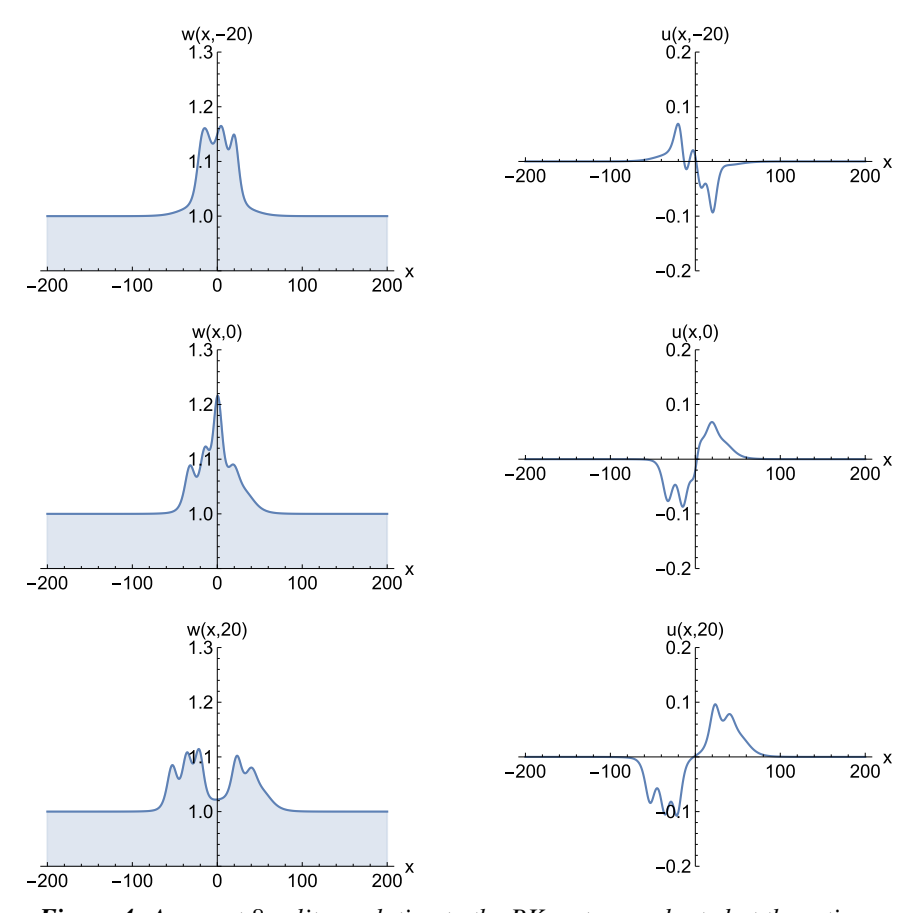


Figure 4. An exact 8-soliton solution to the BK system evaluated at three times

Notice that the errors are most severe near the earliest time for the 8-soliton solution, which is likely due to the edge of a soliton starting to pass out of the interval [-200, 200]. We did not conduct the fourth-order convergence tests, because when evaluating the 8-soliton solution in Mathematica there appeared to be random noise on the order of 10^{-8} introduced in the evaluation of the exact 8-soliton solution, likely due to cut-off error in the calculation of the solution to the system of linear equations. This made it so the smallest possible error in the numerical calculation due to the noise was achieved

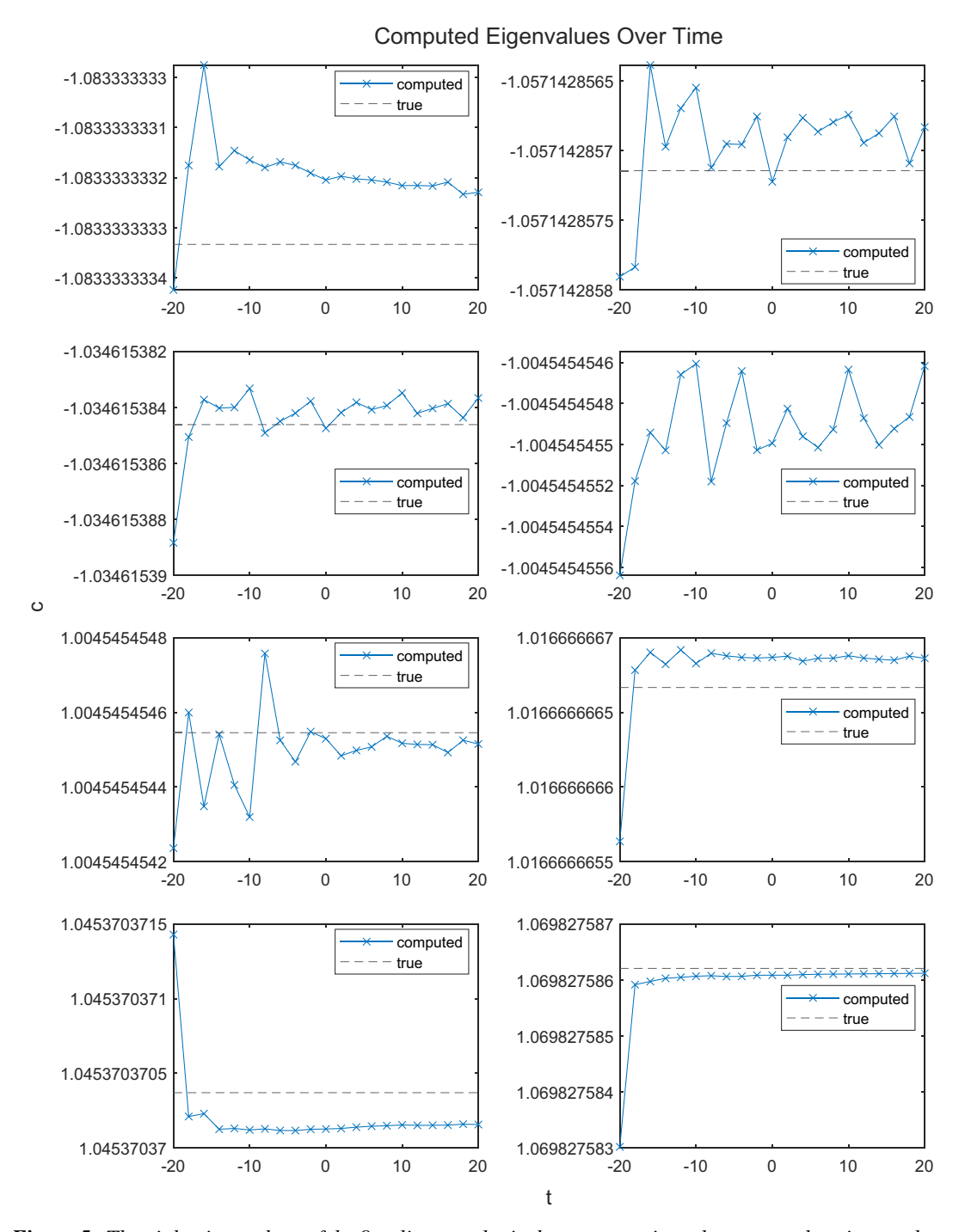


Figure 5. The eight eigenvalues of the 8-soliton synthetic data are consistently computed as time evolves

before the trend could be observed clearly on the log-log plot. However, we note that the error obtained using only a grid spacing of 0.4 has many correct digits, and is likely accurate enough for any practical application in which possible measurement errors could be assumed to be much larger than the error introduced in evaluation of the 8-soliton solution.

6. Conclusion

We presented a numerical method to compute the eigenvalues of the BK system for non-capillary shallow water waves under the physically reasonable assumptions that the particle velocity at the surface satisfies $|v(x)| < 2\sqrt{gh_0}$, and that the surface elevation $\eta(x)$ is bounded. The eigenvalues indicate amplitudes and celerities of potentially hidden left and right-traveling solitons in given data. The envisioned practical application of the method is the analysis of bidirectional shallow-water data. The proposed algorithm is fourth-order accurate, combines bracketing of eigenvalues based on oscillation theory with Newton-Rhapson iterations in order to enable rapid convergence, and is guaranteed to find all eigenvalues. The properties of the method were verified numerically on two *N*-solition solutions of the BK system.

The eigenvalues are only one part of the BK-NFT. We expect that efficient numerical methods to compute the corresponding norming constants and the continuous spectrum can be developed based on the ideas in [35] and [13].

Data availability statement. Data is available from the authors upon request.

Funding statement. This project has received funding from the European Research Council (ERC) under the European Union's Horizon 2020 research and innovation programme (grant agreement No 716669).

Competing interests. None

Ethical standards. The research meets all ethical guidelines, including adherence to the legal requirements of the study country.

Author contributions. Peter J. Prins: Methodology, Software, Validation, Writing – Original Draft; Patrik V. Nabelek: Validation, Figures, Writing – Original Draft, Supervision; Brandon Young: Writing – Review & Editing, Validation, Figures. Sander Wahls: Writing – Review & Editing, Supervision, Project administration, Funding acquisition.

References

- [1] **Ablowitz MJ, Kaup DJ, Newell AC and Segur H** (1974) The inverse scattering transform-Fourier analysis for nonlinear problems. *Studies in Applied Mathematics* **53**, 249–315. https://doi.org/10.1002/sapm1974534249
- [2] Ablowitz MJ and Segur H (1981) Solitons and the Inverse Scattering transform, Philadelphia, PA: SIAM.
- [3] Ali A, Juliussen B-S and Kalisch H Approximate Conservation Laws for an Integrable Boussinesq system, 12. Publisher: EDP Sciences. 1–14. https://doi.org/10.1051/mmnp/201712101 (accessed 16 June 2025).
- [4] Ambrose DM, Bona JL and Milgrom T (2019) Global solutions and ill-posedness for the kaup system and related boussinesg systems. *Indiana University Mathematics Journal* 68, 1173–1198.
- [5] Baeyens T and Van Daele M (2020) The fast and accurate computation of eigenvalues and eigenfunctions of time-independent one-dimensional Schrödinger equations. *Computer Physics Communications* 258, 107568. https://doi.org/10.1016/j.cpc.2020.107568
- [6] Boffetta G and Osborne AR (1992) Computation of the direct scattering transform for the nonlinear Schroedinger equation. Journal of Computational Physics 102, 252–264. https://doi.org/10.1016/0021-9991(92)90370-e.
- [7] Broer L (1975) Approximate equations for long water waves. Applied Scientific Research 31, 377–395. https://doi.org/10. 1007/BF00418048.
- [8] Brühl M and Oumeraci H (2016) Analysis of long-period cosine-wave dispersion in very shallow water using nonlinear Fourier transform based on kdv equation. Applied Ocean Research 61, 81–91. https://doi.org/10.1016/j.apor.2016.09.
- [9] Brühl M, Prins PJ, Ujvary S, Barranco I, Wahls S and Liu PL-F (2022) Comparative analysis of bore propagation over long distances using conventional linear and kdv-based nonlinear fourier transform. Wave Motion 111, 102905. https://doi. org/10.1016/j.wavemoti.2022.102905
- [10] **Byatt-Smith JG** (1971) An integral equation for unsteady surface waves and a comment on the Boussinesq equation. *Journal of Fluid Mechanics* **49**, 625–633. https://doi.org/10.1017/S0022112071002295
- [11] Camassa R, Falqui G, Ortenzi G, Pedroni M and Ho TTV Simple two-Layer Dispersive Models in the Hamiltonian Reduction formalism, 36. Publisher: IOP Publishing. 4523. https://doi.org/10.1088/1361-6544/ace3a0 (accessed 6 October 2024).
- [12] Chekhovskoy I, Medvedev S, Vaseva I, Sedov E and Fedoruk MP (2021) Introducing phase jump tracking-a fast method for eigenvalue evaluation of the direct Zakharov-Shabat problem. Communications in Nonlinear Science and Numerical Simulation 96, 105718. https://doi.org/10.1016/j.cnsns.2021.105718

- [13] Chimmalgi S, Prins PJ and Wahls S (2019) Fast nonlinear Fourier transform algorithms using higher order exponential integrators. IEEE Access 7, 145161–145176. https://doi.org/10.1109/access.2019.2945480
- [14] Christov I (2009) Internal solitary waves in the ocean: Analysis using the periodic, inverse scattering transform. Mathematics and Computers in Simulation 80, 192–201. https://doi.org/10.1016/j.matcom.2009.06.005
- [15] Congy T, El G and Roberti G Soliton gas in Bidirectional Dispersive hydrodynamics, 103. Publisher: American Physical Society. 042201. https://doi.org/10.1103/PhysRevE.103.042201 (accessed 16 June 2025).
- [16] El GA, Grimshaw RHJ and Pavlov MV Integrable shallow-water equations and undular bores 106, 157–186, https://onlinelibrary.wiley.com/doi/pdf/10.1111/1467-9590.00163 _eprint (accessed 16 June 2025).
- [17] **Greenberg L and Babuška I** (1989) A continuous analogue of sturm sequences in the context of sturm–liouville equations. *SIAM Journal on Numerical Analysis* **26**, 920–945. https://doi.org/10.1137/0726051
- [18] Kaup DJ (1975) A higher-order water-wave equation and the method for solving it. Progress of Theoretical Physics 54, 396–408. https://doi.org/10.1143/ptp.54.396
- [19] Klein C and Saut J (2025) On the kaup-broer-kupershmidt systems. EMS Surveys in Mathematical Sciences 12, 215–242. Available at https://doi.org/10.4171/EMSS/98. (accessed 2 October 2024).
- [20] Kupershmidt B (1985) Mathematics of dispersive water waves. Communications in Mathematical Physics 99, 51–73. https://doi.org/10.1007/BF01466593
- [21] Lannes D. The water waves problem. In *Of Mathematical Surveys and Monographs*, American Mathematical Society, 188. Available at https://doi.org/10.1090/surv/188 (accessed 17 June 2025).
- [22] Ledoux V and Daele MV (2010) Solving Sturm-Liouville problems by piecewise perturbation methods, revisited. Computer Physics Communications 181, 1335–1345. https://doi.org/10.1016/j.cpc.2010.03.017
- [23] Ledoux V. (2007). PhD thesis, Ghent University, Study of Special Algorithms for solving Sturm-Liouville and Schrödinger Equations
- [24] Ledoux V and Van Daele M (2010) Solution of Sturm-Liouville problems using modified Neumann schemes. SIAM Journal on Scientific Computing 32, 563–584. https://doi.org/10.1137/090758398
- [25] Lee Y-C and Wahls S (2025) Impact of directional spreading on nonlinear kdv-soliton spectra in intermediate water. Wave Motion 137, 103542. https://doi.org/10.1016/j.wavemoti.2025.103542
- [26] Li Y and Zhang JE (2003) Bidirectional soliton solutions of the classical boussinesq system and AKNS system. Chaos, Solitons & Fractals 16, 271–277. https://doi.org/10.1016/s0960-0779(02)00312-0
- [27] Miles JW (1981) The Korteweg-de Vries equation: a historical essay. *Journal of Fluid Mechanics* 106, 131–147. https://doi.org/10.1017/S0022112081001559
- [28] Nabelek PV and Yim SC. (2024). A nonlinear integrable water-wave system model for gravity and surface-tension waves. in *International Conference on Offshore Mechanics and Arctic Engineering*. American Society of Mechanical Engineers, 87875, V009T12A004. https://doi.org/10.1115/OMAE2024-127034
- [29] Nabelek PV and Zakharov VE (2020) Solutions to the Kaup-Broer system and its (2+1) dimensional integrable generalization via the dressing method. *Physica D: Nonlinear Phenomena* 409, 132478.
- [30] Osborne AR and Bergamasco L (1986) The solitons of zabusky and kruskal revisited: Perspective in terms of the periodic spectral transform. Physica D: Nonlinear Phenomena 18, 26–46. https://doi.org/10.1016/0167-2789(86)90160-0
- [31] Osborne AR (1994) Automatic algorithm for the numerical inverse scattering transform of the Korteweg–de Vries equation. Mathematics and Computers in Simulation 37, 431–450. https://doi.org/10.1016/0378-4754(94)00029-8
- [32] Osborne AR and Petti M (1994) Laboratory-generated, shallow-water surface waves: Analysis using the periodic, inverse scattering transform. *Physics of Fluids* 6, 1727–1744. https://doi.org/10.1063/1.868235
- [33] Osborne AR, Segre E, Boffetta G and Cavaleri L (1991) Soliton basis states in shallow-water ocean surface waves. Physical Review Letters 67, 592. https://doi.org/10.1103/PhysRevLett.67.592
- [34] **Prüfer H** (1926) Neue Herleitung der Sturm-Liouvilleschen Reihenentwicklung stetiger Funktionen. *Mathematische Annalen* **95**, 499–518. https://doi.org/10.1007/bf01206624
- [35] Prins PJ and Wahls S (2019) Soliton phase shift calculation for the Korteweg-de Vries equation. IEEE Access 7, 122914–122930.
- [36] Prins PJ and Wahls S (2022) Reliable computation of the eigenvalues of the discrete kdv spectrum. Applied Mathematics and Computation 433, 127361. https://doi.org/10.1016/j.amc.2022.127361
- [37] Pryce JD. 1993. Numerical solution of Sturm-Liouville Problems. Monographs on Numerical Analysis, Oxford Science Publications, Clarendon Press.
- [38] Redor I, Barthélemy E, Michallet H, Onorato M and Mordant N (2019) Experimental evidence of a hydrodynamic soliton gas. Physical Review Letters 122, 214502. https://doi.org/10.1103/PhysRevLett.122.214502
- [39] Sachs RL (1988) On the integrable variant of the Boussinesq system: Painlevé property, rational solutions, a related many-body system, and equivalence with the AKNS hierarchy. *Physica D: Nonlinear Phenomena* 30, 1–27. https://doi.org/10.1016/0167-2789(88)90095-4
- [40] Suret P, Randoux S, Gelash A, Agafontsev D, Doyon B and El G (2024) Soliton gas: Theory, numerics, and experiments. *Physical Review E* 109, 061001.
- [41] Teutsch I, Brühl M, Weisse R and Wahls S (2023) Contribution of solitons to enhanced rogue wave occurrence in shallow depths: a case study in the southern North Sea. Natural Hazards and Earth System Sciences 23, 2053–2073. https://doi.org/ 10.5194/nhess-23-2053-2023

- [42] Teutsch I, Weisse R and Wahls S (2023) Brief communication: Implications of outstanding solitons for the occurrence of rogue waves at two additional sites in the north sea. Natural Hazards and Earth System Sciences Discussions 2023, 1–8. https://doi.org/10.5194/nhess-24-2065-2024
- [43] Trillo S, Deng G, Biondini G, Klein M, Clauss G, Chabchoub A and Onorato M (2016) Experimental observation and theoretical description of multisoliton fission in shallow water. *Physical Review Letters* 117, 144102. https://doi.org/10. 1103/PhysRevLett.117.144102
- [44] Vasylchenkova A, Prilepsky JE and Turitsyn SK (2018) Contour integrals for numerical computation of discrete eigenvalues in the zakharov–shabat problem. *Optics Letters* 43, 3690–3693. https://doi.org/10.1364/OL.43.003690
- [45] Wahls S and Poor HV. (2013). Introducing the fast nonlinear fourier transform. In 2013 IEEE International Conference on Acoustics, Speech and Signal Processing. IEEE, 5780–5784. https://doi.org/10.1109/ICASSP.2013.6638772
- [46] Wu TYt (1995) Bidirectional soliton street. Acta Mechanica Sinica 11, 289–306. https://doi.org/10.1007/bf02488837
- [47] Zhang JE and Li Y (2003) Bidirectional solitons on water. Physical Review E 67, 016306. https://doi.org/10.1103/ PhysRevE.67.016306